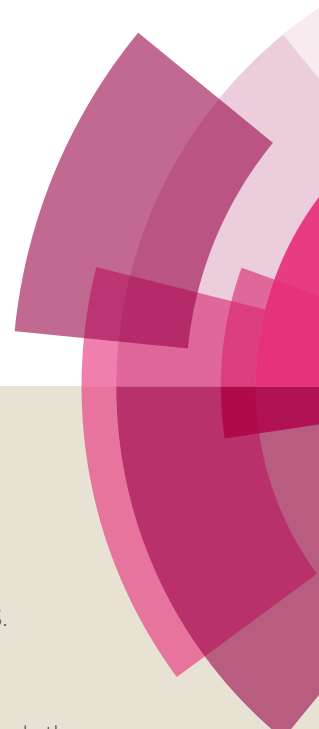


NJC

Accepted Manuscript



This article can be cited before page numbers have been issued, to do this please use: N. Bouzayani, S. MARQUE, B. Djelassi, Y. Kacem, J. Marrot and B. Ben Hassine, *New J. Chem.*, 2018, DOI: 10.1039/C7NJ04597B.



This is an Accepted Manuscript, which has been through the Royal Society of Chemistry peer review process and has been accepted for publication.

Accepted Manuscripts are published online shortly after acceptance, before technical editing, formatting and proof reading. Using this free service, authors can make their results available to the community, in citable form, before we publish the edited article. We will replace this Accepted Manuscript with the edited and formatted Advance Article as soon as it is available.

You can find more information about Accepted Manuscripts in the [author guidelines](#).

Please note that technical editing may introduce minor changes to the text and/or graphics, which may alter content. The journal's standard [Terms & Conditions](#) and the ethical guidelines, outlined in our [author and reviewer resource centre](#), still apply. In no event shall the Royal Society of Chemistry be held responsible for any errors or omissions in this Accepted Manuscript or any consequences arising from the use of any information it contains.



NJC

PAPER

Enantiopure Schiff bases of aminoacid phenylhydrazides: impact of the hydrazide function on their structure and properties

Nadia Bouzayani,^a Sylvain Marque,^{b*} Brahim Djelassi,^c Yakdhane Kacem,^{a*} Jérôme Marrot^b and Béchir Ben Hassine^a

Received 00th November 2017,
Accepted 00th January 20xx

DOI: 10.1039/x0xx00000x

www.rsc.org/

A rapid and eco-friendly synthesis of new enantiopure Schiff bases **5a-e** was performed from various α -amino acid phenylhydrazides and 2-hydroxynaphthaldehyde using microwave or ultrasound irradiation in yields ranging from 57 to 75%. These imines were characterized using ^1H & ^{13}C NMR, FTIR, mass and UV-vis spectroscopies. In addition, the solid state molecular structure of **5b** was determined by single crystal X-ray diffraction which shows that this compound adopts the zwitterionic form, crystallizing in the non-centrosymmetric orthorhombic system with the space group $P2_12_12_1$. DFT calculations show that the BMK/6-31G(2df,2pd) method in the gas phase is well adapted to describe the geometry of the solid state. Theoretical results corroborate the ionic character of this species in concordance with spectroscopic results and lead to a new thin description. The Schiff bases **5a-e** behave as organic semiconductors with the $E_{\text{og}} \approx 2.77$ eV. The *in-vitro* antibacterial study showed that these molecules exhibited various levels of antibacterial effect against all the tested bacterial strains.

1. Introduction

Schiff bases¹ have been studied due to their significant properties in various fields²⁻⁶. During the last years, they have received great attention from scientists worldwide due to their ease of synthesis, as precursors for the preparation of biologically active compounds⁷⁻¹¹, especially imines bearing electron-withdrawing N-substituents which are useful intermediates and building blocks in the construction of bactericidal, fungicidal and anti-inflammatory agents.^{12, 13} Schiff bases are among the most versatile and useful ligands and their metal complexes have been widely used as catalysts for many organic reactions.¹⁴⁻¹⁷ Some salicyl-methanimine-like compounds present interesting mechanical-, thermo- or photo- chromic behaviours for their capacity to undergo tautomerism prototropic and many reports on the equilibrium have recently been described in the literature.¹⁸⁻²⁰ It is worth noting that Schiff bases can appear under numerous forms (Figure 1). For some examples the structure and properties have been investigated in relationship to the forms (or the mix of the forms); the results were strongly dependent on the electronic environment by the substituents on the aromatic group or on the nitrogenated pendant arm,²¹ the addition of

supplementary functions²² which favors a species in regard to another, or else of the physical state²³, the solvent¹⁹ or the temperature²⁵ (Table 1). The work-up revealed sometimes crucial to isolate the compounds even in the solid state²⁶. Thus, the table 1 revealed as soon as a slight modification on the skeleton is operated,²⁷ the resulting structure is deeply impacted and a new elucidation needs to be performed. Moreover, when comparisons with calculations exist, the choice of the method and of the basis set appears rarely investigated in the literature and never clear-cut demonstrated. Considering the above subjects with our studies on green-organic synthesis and the reactivity of α -aminoacid phenylhydrazides^{28, 29} derived from (L)- α -aminoacids herein, is reported a simple and rapid method for the preparation of chiral Schiff bases from the coupling of phenylhydrazides with 2-hydroxynaphthaldehyde under solvent-free conditions. The fine characterization of these new compounds is realized to investigate the influence of both the aminoacid and the hydrazide function on the structure at solid and liquid states. These data are firmly compared to quantum chemical calculations and highlight a new and most granular description of these structures.

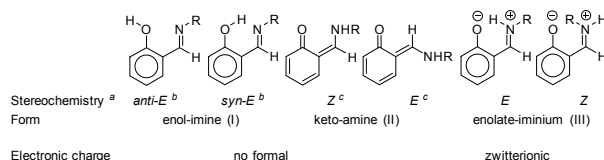


Fig. 1. Representation of monomeric forms^d. ^a Representations of localized π -aromatic electrons are possible doubling each I and III drawn forms; ^b the Z configuration of enol-imine forms is not reported in literature; ^c *syn* and *anti* conformations could be also defined for the keto-amine forms according to the spatial position of N-H and N-R in

^a Laboratoire de Synthèse Organique Asymétrique et Catalyse Homogène, (UR 11ES56) Université de Monastir, Faculté des Sciences de Monastir, avenue de l'environnement, Monastir 5000, Tunisie. Fax: (+216) 73 500 278; Tel: (+216) 73 500 275. E-mail: kacem.yakhane@fphm.rnu.tn

^b Université de Versailles, Saint-Quentin-en-Yvelines, Institut Lavoisier de Versailles (ILV), UMR CNRS 8180, 45 avenue des Etats-Unis, 78035 Versailles, France. E-mail: sylvain.marque@uvsq.fr

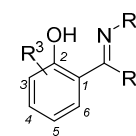
^c Laboratoire des maladies transmissibles et substances biologiquement actives, Faculté de Pharmacie, Rue Avicenne 5000 Monastir, Tunisie.

Electronic Supplementary Information (ESI) available: Cartesian coordinates and properties of species for calculations, UV spectroscopy method, crystallographic data and comparison with Schiff bases of the literature, NMR spectra. See DOI: 10.1039/x0xx00000x

regard the oxygen atom; ^d lot of reported studies do not distinguish the forms II and III (mesomeric forms).

Table 1. Selected examples of Schiff bases in the literature (for a more complete comparison see SI).

Entry	R ¹	R ²	R ³	Physical state	Form	Ref
1	H	Me, alkyl	4-OMe	solid	II-Z	27
2	H	Ph or Bn	4-OMe	solid	I	27
3	H	Ph	3,5-di- <i>t</i> -Bu	<i>i</i> -Pent	I (from 77 to 297 K)	25
3	H	Ph	H	<i>i</i> -Pent	I (rt) II (<140K)	25
4	Me	CH ₂ CH ₂ OH	H	solid	II	19
5	H	CH ₂ CH ₂ OH	H	MeOH or EtOH	I minor / II major	19
6	H	CH ₂ CH ₂ OH	H	Tol or DMF	I very major	19
7	H	CH ₂ CH ₂ SO ₃ ⁻ K ⁺	3-OMe	solid	I-E / II-Z	20
8	H	CH ₂ CH ₂ SO ₃ ⁻ K ⁺	3-OMe	MeOH	I / II	20
9	H	CH ₂ CH ₂ SO ₃ ⁻ K ⁺	3-OMe	DMSO	I	20



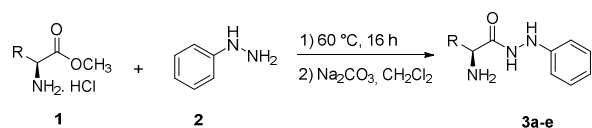
2. Results and discussion

2.1 Synthesis.

The starting α -amino acid phenylhydrazides^{29, 30} **3** were obtained under mild conditions from the commercially available (L)- α -amino acid ester hydrochlorides **1a-e** and the phenylhydrazine **2** at 60 °C during 16 h in good yields (Scheme 1). The condensation of (L)-alanine phenylhydrazide with the 2-hydroxy-1-naphthaldehyde **4** was studied as a model reaction to provide compound **5a** (Scheme 2). The reaction was first examined under catalytic conditions with different solvents (Table 2).

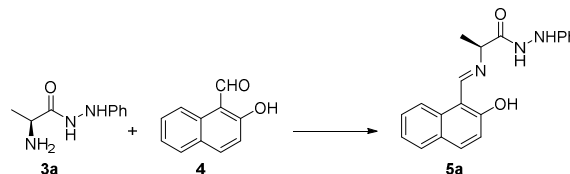
First, we thought to study the effect of temperature because the reactants, especially the 2-hydroxy-1-naphthaldehyde, have a poor solubility at room temperature in the majority of solvents (toluene, EtOH...). Nevertheless, employing of high reaction temperature (100 °C) with 1 mol% of sulfuric acid as catalyst during 10 h, no formation of the desired product was observed (entry 1). The reaction performed with 1 mol% of paratoluenesulfonic acid as catalyst in methanol during 14 h at 65 °C allowed obtaining the compound **5a** with a low yield (entry 2) due to the formation of degradation products. This is explained by the formation of salts that causes the weakening of yields. A further decrease of the reaction temperature to 50 °C and the reaction time to 4 h without catalyst gave the desired coupling product and allowed to increase the yield to 70% (entry 3).

No conventional heating was explored performing the reaction under ultrasound activation in methanol at room temperature (Scheme 3 and Table 2, entry 4). The product **5a** was obtained with good yield after 20 min while the reaction performed under microwave activation was completed in only 5 min (entry 5). The Table 3 presents the synthesized Schiff bases **5a-e** yielded from 57 to 75 %.



R = Me (**3a**), *i*-Pr (**3b**), *i*-Bu (**3c**), Bn (**3d**), CH₂-OH (**3e**)

Scheme 1. Synthesis of the α -amino acid phenylhydrazides **3a-e**.



Scheme 2. Coupling of the 2-hydroxy-1-naphthaldehyde **4** with (L)-alanine phenylhydrazide **3a**.

Table 2. Optimization of the reaction conditions for the coupling of the 2-hydroxy-1-naphthaldehyde **4** and (L)-alanine phenylhydrazide **3a**.

Entry	Catalyst	Temperature	Time	Solvent	Yields
1	H ₂ SO ₄ (1)	100	10	Toluene	NR ^a
2	PTSA (1)	65	14	MeOH	20
3	-	50	4	MeOH	70 ^b
4	-	rt	20 min	MeOH	71 ^c
5	-	100	5 min	-	71 ^d

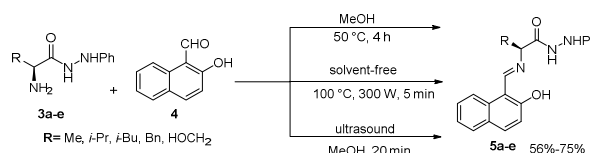
^a No reaction was occurred.

^b Conditions: (L)-alanine phenylhydrazide (10 mmol), 2-hydroxynaphthaldehyde (10 mmol), under argon.

^c Ultrasound irradiation.

^d Microwave irradiation (startSYNTH).

It was noted that no racemization of the asymmetric carbon atom of phenylhydrazide was occurring, based on published reports^{28, 29} that showed no epimerization was observed when mild conditions were used. We observed that products **5a-e** can not be purified by chromatography but they are stable in air for several months at room temperature.



Scheme 3. Synthesis of Schiff bases **5a-e**.

Table 3. Coupling of the 2-hydroxy-1-naphthaldehyde **4** and phenylhydrazides **3a-e**.

Entry	Product	Yields Δ^a	Yields MW ^b	Yields)) ^c
1	5a (Me)	70	71	71
2	5b (<i>i</i> -Pr)	67	69	68
3	5c (<i>i</i> -Bu)	70	74	72
4	5d (Bn)	56	60	57
5	5e (HOCH ₂)	73	75	72

^a Conditions: α -amino acid phenylhydrazide (10 mmol), 2-hydroxynaphthaldehyde (10 mmol), MeOH, 4 h under argon.

^b Conditions of activation: microwave irradiation (startSYNTH), 100 °C, 5 min.

^c Conditions of activation: ultrasound irradiation, rt, 20 min.

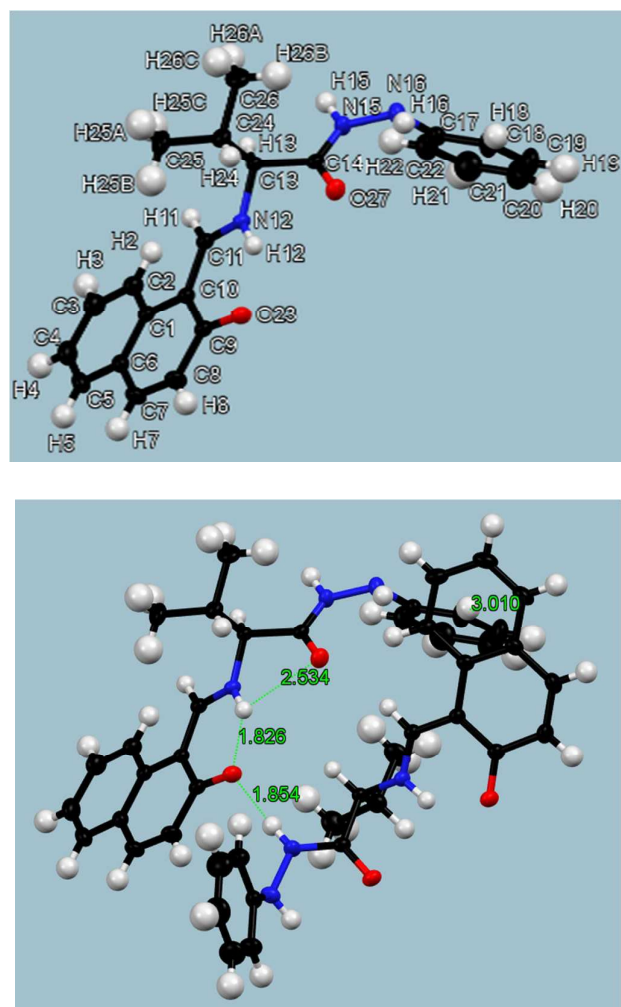


Fig. 2. X-ray analyses (anisotropic displacement ellipsoids pictured are set at 30% probability): a) ORTEP of **5b** (up); b) supramolecular structure (down).

2.2 Solid state study.

Single crystal X-ray diffraction measurements for **5b** were carried out at $T = 200$ K with a Bruker D8 VENTURE diffractometer equipped with a PHOTON 100 CMOS bidimensional detector using a high brilliance μ S microfocus X-ray Mo $K\alpha$ monochromatized radiation ($\lambda = 0.71073$ Å). An empirical absorption correction was applied using the SADABS program^{31a} based on the method of Blessing.^{31b} The structure was solved by direct methods and refined by full-matrix least squares using the SHELX-TL package.^{31c,d} The hydrogen atoms were placed from the electron density in calculated positions and were included in the refinement without restraint on the nitrogen atoms. Crystal data^{31e} of **5b** are given in supporting information, while ORTEP is presented in Figure 2 and the selected geometrical parameters are listed in the table 5. Molecular graphics were generated by Mercury 3.9.^{31f} In contrast to the several Schiff bases of literature, **5b** crystallized in a unique space group $P2_12_12_1$. No desmotropic forms were observed. In the crystal structure, the succession

of oxygen, nitrogen, and acidic H atoms bring numerous intramolecular electrostatic interactions. Thus, the O(23)-C(9)-C(11)-N(12), and C(11)-N(12)-C(14)-N(15) and O(27)-C(14)-N(15)-N(16) dihedral angles of respectively $-3.5(1)^\circ$, $+0.2(3)^\circ$ and $-7.9(2)^\circ$ indicated that the geometry is very close to the planarity on a large region of the molecule. In the packing of crystal structure **5b**, intermolecular O(23)...H(15)-N(15) hydrogen bonding contact of 1.85(2) Å is formed due to the presence of the hydrazide function sustaining the supramolecular framework (figure 2b). Interestingly, structures show one medium weak (O(27)...H(12)-N(12) with 2.53(2) Å) and two strengths (N(12)-H(12)...O(23) with 1.83(2) Å & O(23)...H(15)-N(15) with 1.85(2) Å) hydrogen bonds. This last intermolecular hydrogen bond is so strength that the C(9)-O(23) bond is slightly distorted with an O(23)-C(9)-C(10)-C(1) dihedral angle bond of $175.0(1)^\circ$. Moreover, the supramolecular structure is reinforced by the H- π interaction between the phenyl and naphthyl groups with a 3.010 Å value from H to centroid. In order to elucidate the fineness of the structure between the forms II and III, the bonds C(9)-O(23) and C(11)-N(12) were measured with values of 1.279(2) Å and 1.307(2) Å respectively. The value of CN bonding length is in full agreement with a III shaped writing, whereas the CO bond denotes a character between simple and double bond.³² Therefore, three intra and intermolecular hydrogen bonds determine the structure around the nitrogen N(12) as a (*E*)-III liked form, but around the oxygen O(23) an intermediate view between (*E*)-III and the *anti*-(*Z*)-II ketoamine forms is a more accurate of writing.

2.3 Solution NMR study.

The compounds **5a-e** were found to have very poor solubility in common organic solvents including dichloromethane, chloroform, toluene, ethyl acetate and tetrahydrofuran but they were soluble in polar solvents such as methanol, acetonitrile, *N,N*-dimethylformamide and dimethylsulfoxide. In general, Schiff bases in solution can exhibit several possible tautomeric forms: as C-O-H...NCH in enol imino (I)³³ and C=O...H-NCH in keto-amino (II) tautomers.³⁴ In solution ¹H NMR, the characterization supported by the H(12) proton is rarely a relevant argue, since chemical shifts show a high solvent dependency.^{26, 35} Moreover, the hydrazide protons are also sensitive to the deuterium exchange. Hence, H(12) and hydrazide protons are unobserved in MeOD-*d*₄ even sometimes for both in CDCl₃³⁵⁻³⁷. The chemical shift of the H(11) iminomethine proton does not give no more information in itself as well.³⁸ Nevertheless, ¹³C NMR spectroscopy in solution clearly makes it possible to qualify the nature of the C(9) atom as phenolic or “quinodic” carbon (often presented as such regardless of forms II or III which it belongs).³⁹ For the compounds **5a**, **5b**, **5d** and **5e** recorded in MeOD-*d*₄, signals were observed at 178.1, 177.6, 177.1, and 175.5 ppm respectively, and then at 166.5 ppm for **5c** recorded in CDCl₃. These values show the quinodic nature of the carbon C(9) in methanol at room temperature and place the position of the H(12) atom on the nitrogen N(12), although a small amount of

the phenolic form can be sometimes observed in the ^1H NMR spectrum (less than 10%). In the chloroform, only one signal was found above 170 ppm for **5c** with a value of 171.5 ppm ascribed to the C(14) hydrazide carbon usually at 173–174 ppm in CDCl_3 or $\text{MeOD-}d_4$ ^{28, 29} in full agreement with the literature data.⁴⁰ Thus, the signal at 166.5 ppm reveals the phenolic behaviour of the carbon in complete concordance with the usual observed value in this solvent.³⁹ Interestingly, the ^1H NMR spectrum in CDCl_3 depicts a signal above 14 ppm, although the value³⁸ does not prove in itself the presence of the phenolic proton for **5c**. The iminomethine carbon (C11) was observed at 159.7, 160.5, 160.1, 161.2 in $\text{MeOD-}d_4$ for **5a**, **5b**, **5d**, **5e** respectively, and then 162.2 ppm in CDCl_3 for **5c**. These values illustrate the imino character³⁹ (protonated or not) around the nitrogen N12.

NMR experiments were pursued in $\text{DMSO-}d_6$ with **5b**, **5c** and **5e** then three labile protons were observed with an interaction (COSY) between the two NH of hydrazide function allowing to ascertain the attribution at about 3.37 ppm to the H(12) in association with the residual water. The ^{13}C NMR spectrum indicated that C(9) and C(11) resonate at approximately 175 and 159 ppm respectively indicating a full quinoidic character as well as the presence of a well-marked iminium function.³⁹ This result in DMSO solution joins the conclusions of the solid state with a III liked form around the nitrogen N(12) and a II ketoamine form around the oxygen O(23). A series of NOESY experiments was performed in order to gain insight into the geometry. The correlation between H(2) and the H(11) protons show a Z stereochemistry relationship of the C=N bond, with a respect of a II-shaped writing, regardless for $\text{DMSO-}d_6$ or $\text{MeOD-}d_4$.

At this stage, room temperature NMR experiments allow certify the exclusive (or very major) formation in methanol of the *anti*-(Z)-II structure around the oxygen and (*E*)-III iminium around the nitrogen. It is quite surprising since usually the phenolic form is the exclusive one in agreement with the polarity of this solvent. The presence of the hydrazide function, bringing a second intramolecular bond, is likely responsible for this astonished result. In chloroform, the I enol-imine can be sighted almost as the sole form; in dimethylsulfoxide the results are very close to the crystallographic data: (*E*)-III iminium and *anti*-(Z)-II quinoidic forms the environment of N(12) and O(23) respectively.

2.4 Infrared Spectroscopy.

Neat solid FT-IR spectra of the compounds **5a-e** were recorded in the 3500–600 cm^{-1} region and some characteristic stretching vibration modes can be identified in this area. In contrast with ^{13}C NMR, CO function is usually not an essential parameter to identify the I, II or III forms since C=O and C=N bands give similar contribution to the concomitant wavelength,^{41, 42} especially if the both enol-imine(I) and keto-amine(II) are present¹⁹. However, in our cases the hydrazide function deeply impacts the H(12) proton, as stated by the X-ray results, to get unusual data. Indeed, the IR spectra of **5a-e** depicted strong bands observed at 1625, 1616, 1625, 1617 and 1693 cm^{-1}

respectively, which are attributed to the vibration of C=O bands and besides, sharp bands appeared in respectively 1544, 1543, 1546, 1545 and 1542 cm^{-1} corresponding to the stretching vibrations of (C=N) bands. It refines at the solid state the presence of the keto-amine form II or its mesomeric form III.

Interestingly, the C=O of the hydrazide function absorb at 1667, 1654, 1677(d), 1675, 1693 cm^{-1} for **5a-e**⁴³ that would be difficult to attribute and confusing because of the C=O quinoidic form^{42b}. The IR spectra of **5a-e** show broad bands centred at around 2981, 2788, 2950, 2746 and 2680 cm^{-1} , due to $\nu(\text{HN}^+)$ modes as a result of intramolecular hydrogen bonds $\text{N}^+\text{H}\cdots\text{O}$ which are usually very strong. All of the Schiff bases **5a-e** in the present investigation exhibit a broadband at 3334, 3332, 3184, 3341 and 3313 cm^{-1} assigned to $\nu_{\text{N-H}}$ vibrations; but once more, these ones can be easily confused with $\nu_{\text{O-H}}$.^{41b, 42a} To have a fruitfully understanding, the out-of-plane $\gamma_{\text{C-O}}$ band needs to be checked. **5b** absorbs with thin bandwidths at 843 and 872 cm^{-1} where the two enol-imine and keto-amine coexist, although apparently contradictory to the crystallographic data. However, it is known²⁶ that a slight mechanical treatment transforms the keto-amine to the enol-imine forms evidencing a solid state reactivity.

2.5 Electronic absorption spectroscopy.

The optical properties of compounds **5a-e** were investigated using UV/vis absorption studies in a dilute (10^{-6} M) acetonitrile solution in the range 308–600 nm, displayed in figure 4. UV spectra exhibit from three up to four bands in the visible wavelengths: about 423, 403, 363 and 350 nm (Table 4). The absorption band at 403 nm, arises from intermolecular $\pi\text{-}\pi^*$ transitions. The highest λ_{max} value with intense absorption gives access to a roughly HOMO-LUMO electronic transition, evaluated by the extrapolation of the tangent to the first inflexion point. The table 4 presents herewith the optical gap energies evaluated around of $E_{\text{og}} = 2.77$ eV, corresponding to a semiconductor behaviour for these Schiff bases.

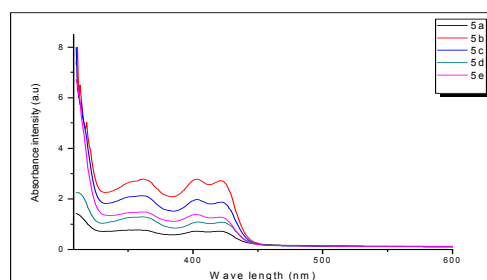


Fig. 3. The UV-Vis spectra of the Schiff bases **5a-e** in MeCN solution (10^{-6} M) at rt.

Table 4. Optical properties of the chiral compounds **5a-e**.^a

Entry	Compound	λ_{max}	λ_{gap}	E_{og}
1	5a	423.31, 400.49, 364.74, 341.19	447.65	2.77
2	5b	423.31, 403.25; 363.13, 350.25	449.27	2.76
3	5c	423.31, 403.54, 363.21, 350.28	447.65	2.77
4	5d	424.04, 403.54, 363.21, 348.81	450.90	2.75
5	5e	423.31, 401.22, 364.00, 350.28	447.65	2.77

^a λ values are given in nm; energies are given in eV.

2.6 Calculations.

Method calculations and basis sets

The restraint free geometry optimization of species was performed using the Gaussian 09 software⁴⁴ with standard parameters and a tight criteria of convergence. The determination of structures in solution was carried out using the self-consistent reaction field (SCRF) method. Transition states were located without constraint along their corresponding reaction pathways, characterized by a sole imaginary frequency, checking out the connection with the ground and final states. Final predicted energies included the zero-point vibrational and thermal energy corrections at 298.15 K (see SI), giving the Gibbs free energy in the both gas phase and solvent solution for minima and maxima of the potential electrostatic surface. The molecule **5b** was chosen as a model and the Cartesian coordinates obtained by X-ray data were used as starting point for the geometrical optimization. Several geometrical parameters (distances, angles and dihedral angles, see figure 2a) of the species **5b** including crucial nitrogen and oxygen atoms, especially charged atoms were selected to appreciate the relevance of the calculated geometries. The relative difference between calculated and experimental values was evaluated over the whole parameters; Hartree-Fock (HF) and DFT methods were tested in the gas phase and results summarized in the Table S4 (see ESI).

First attempts HF and DFT-B3LYP⁴⁵ methods were tested for the screening of the basis sets (entries 1-10). Surprisingly 3-21G gave good results with both HF and B3LYP methods to approach the more accurate values of the geometrical parameters (entries 1 and 6). However to take into account the electronic dispersion for further calculations (pathways and properties), a more extended basis set was required. Thus, diffuse (+) and polarized (d and/or p) functions were added on hydrogen or heavy atoms. Several DFT methods were tested (entries 10-21). By example, the M062X DFT method⁴⁶ (entry 15) underestimates the hydrogen bonds in favour of a combination of the approaches of the two aromatic groups without π -stacking interactions being strongly stated, the resulting structure is so clearly different of the X-ray data. Unexpectedly, DFT methods including dispersion terms and long range correction CAM-B3LYP⁴⁷ were not better than the classic ones (entries 19 and 21). Although PBE1PBE,⁴⁸ ω B97XD⁴⁹ and B3P86⁵⁰ methods (entries 11, 16 and 21), often used in the literature, gave correct results but were not the best methods to describe the geometry. BMK⁵¹ was clearly found as the full adequate DFT method to reach the geometry of the structure (entry 14).

Fixing the BMK DFT method, basis sets were established (entries 22-32). Once more 3-21G was found as the basis set the closer of the X-ray data to get the most accurate value of bond length; angle values are acceptable as well, but dihedral angle values were enough different from the crystallographic data leading to a high value of the MAD (entry 22). Triple-split valence zeta basis are not better sets than double-split valence ones (compare entries 23 with 25, 24 with 26). Full (D95, entry 29) or valence (D95V, entry 30) double-zeta basis of

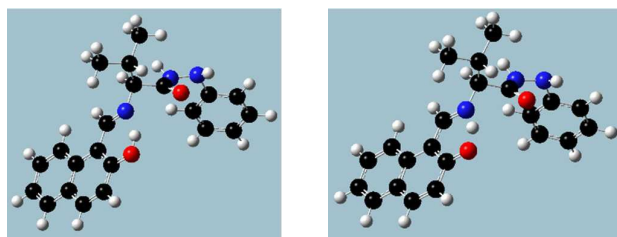
Dunning/Huzinaga⁵² gave poor results. Basis including diffuse functions gave unsatisfactory results (entries 27 and 28). Diffuse functions are used for atoms with high number of electrons and anions but give bad results for cations. Indeed, the part charged negatively should be roughly dispersed in the aromatic cycle, whereas the part charged positively would be very localized on the nitrogen due to the iminium form; the cationic character prevails over the anionic one.

To summarize, the employment of a very high angular moment basis is not needed to reach an accurate geometry and brings only very few enhancements in results towards of moderately polarized functions. Thus, the use of heavy basis sets appears interesting only with the aim at studying chemical pathways or getting properties. Finally, an optimization at a BMK/6-31G(2df,2pd) is the best compromise in terms of computational time and high level of accuracy to successfully investigate the potential energy surface with the geometrical minima, the transition state and the physical properties.

Static approach

The geometry is quite similar between the crystallographic data and the gas phase (Figure 4). A notable difference is the more important planarity in the gas phase concerning the naphthyl cycle and its close heavy adjacent atoms. In fact, in the sole molecule the dihedral angles O(23)-C(9)-C(10)-C(11) and C(9)-C(10)-C(11)-N(12) are -3° and $+3^\circ$ respectively (vs $-9.9(2)^\circ$ and $+5.8(2)^\circ$ for the solid state). This gap with the gas phase can likely be attributed to the supramolecular electrostatic stack, which contributes to twist the more ionic region (Figure 2b). A singular point is the presence of a second intramolecular hydrogen bond inherent to the hydrazide function. Consequently, two labile hydrogens are approximately aligned with one oxygen atom with an H(12)-C(14)-O(27)-H(16) dihedral angle of $169.0(7)^\circ$ leading to an increased rigidification of the conformation. The position of the amino acid residue is placed to minimize the electrostatic repulsion with the hydrazide function and the enolate-iminium part (Figure 5). Thus, the isopropyl group is considered such as the bulky group where the both methyls do not superpose to the nitrogen- and oxygen-containing region that is to say the hydrogen (H24) is oriented above it and the two methyl groups at the opposite. Curiously, the spatial arrangement of the phenyl group is close to those of the solid state revealing that the intermolecular H- π interaction in the solid state (*vide supra*) is not essential to maintain its conformation.

The examination of the charge distribution is fruitful in the gas phase (table 5). The anionic character of O(23) is clearly evidenced whatever the model is, with the adjacent carbon C(9) which offsets this charge showing a phenolic behaviour of the CO bond (entries 1 and 2). The nitrogen N(12) bears also a partial negative charge and the hydrogen H(12) can be therefore considered as its counter ion (entries 5 and 6). Atoms C(10) and C(11) are less affected, but have a distribution of charges in agreement with the expected writing for mesomeric forms (entries 3 and 4). To sum up, although the geometries are very close, the ionic character in the gas phase is more expressed than in solid one.

Figure 4. Optimized geometries at a BMK/6-31G(2df,2pd) level in the gas phase for **5b**: enol-imine form (left) and TS from one form to another (right).

Dynamic approach

Using the BMK/6-31G(2df,2pd) method and basis set in the gas phase, the **5b** enol-imino form was found 2.4 kJ.mol⁻¹ less stable than the keto-amino one (Figure 4). The transition state (TS) from the keto-amino to the enol-imine was located with a barrier energy of $\Delta G^\ddagger = 9.7$ kJ.mol⁻¹. The hydrogen bonding N(12)...H...O(23) in the TS rises to the equal distance values between nitrogen and oxygen atoms (1.218 and 1.249 Å) then changes in the enol form (N...H-O) with 1.698 and 0.989 Å. Besides, the hydrazide second intramolecular hydrogen bonding is moving from the keto-amino form 2.818, to 2.289 in TS and up to 2.273 Å for the enol-imine showing the deep involvement in the H transfer but without affecting the coexistence of this second hydrogen bond.

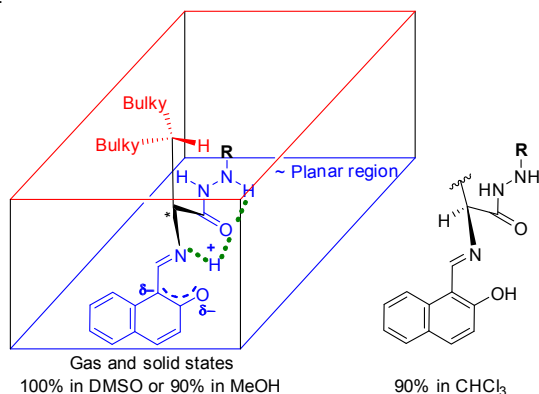
Table 5. Selected values for the charge distribution of **5b** in the gas phase.^a

Entry	Atom	Atomic charge model			
		Mulliken ^b	Natural ^b	ESP-derived	
				CHelpG scheme ^c	MK scheme ^c
1	O(23)	-0.43	-0.59	-0.60	-0.53
2	C(9)	0.31	0.44	0.66	0.57
3	C(10)	-0.17	-0.23	-0.31	-0.39
4	C(11)	0.04	0.13	0.14	0.07
5	N(12)	-0.31	-0.54	-0.32	-0.09
6	H(12)	0.32	0.46	0.35	0.31

^a Calculated at a MP2/6-31G(2df,2pd) on the BMK/6-31G(2df,2pd) optimized geometry, see ESI for more details.

^b Mulliken⁵³ or natural population⁵⁴ analyses.

^c Electrostatic potential (ESP)-derived charges using the CHelpG⁵⁵ or Merz-Kollman-Singh⁵⁶ schemes.

Figure 5. Synoptic of the thin description of the Schiff bases according to the physical state.**Table 6.** Minimum inhibitory concentration (MIC) and minimum bacterial concentration (MBC) in mg/mL of the compounds **5a-e** against selected bacteria.

Entry	Cmpd	<i>E. coli</i>	<i>S. aureus</i>	Ca	S.E	P.S	B.S
		MIC MBC	MIC MBC	MIC MBC	MIC MBC	MIC MBC	MIC MBC
1	5a	0.18	0.18	0.37	0.37	0.37	0.37
		0.37	0.37	0.37	0.37	0.37	0.37
2	5b	1.5	1.5	1.5	1.5	1.5	0.75
		1.5	1.5	1.5	1.5	1.5	0.75
3	5c	1.5	1.5	1.5	1.5	1.5	0.75
		1.5	1.5	1.5	1.5	1.5	0.75
4	5d	1.5	1.5	1.5	0.75	1.5	0.75
		1.5	1.5	1.5	1.5	1.5	0.75
5	5e	1.5	1.5	1.5	0.75	1.5	0.75
		1.5	1.5	1.5	1.5	1.5	0.75

E. coli: *Escherichia coli*, *S. aureus*: *Staphylococcus aureus*, Ca: *Candida albicans*, S.E: *Salmonella enteridis*, P.S: *Pseudomonas aeruginosa*, B.S: *Bacillus subtilis*

2.7 Biological activity.

First, analgesic activity of all the Schiff bases was tested *in vivo* using the carrageenan-induced rat paw oedema test. Unfortunately, no analgesic activity was observed. The synthesized Schiff bases were screened against microorganisms such as *E. coli*, *S. aureus*, *B. subtilis*, *Candida albicans*, *Salmonella enteridis* and *Pseudomonas aeruginosa* to assess their potential as antimicrobial agent. The antibacterial activity was evaluated using the Disc Diffusion method. The stock solution of the test compound was prepared by dissolving 3 mg of the test compound in 1 mL of DMSO solvent. The bacteria were subcultured in agar medium. The petri dishes were incubated for 24 h at 37 °C. Gentamycine was also screened under similar conditions as the reference drug. The zones of inhibition based upon zone size around the discs were taken approximately. The minimum inhibitory concentration was determined using the microdilution method. It was defined as the lowest concentration of the tested product that completely suppresses cell growth. However, a Minimal Bactericidal Concentration (MBC) was defined as the lowest concentration of the extract that kills 99.99% of the tested bacteria.⁵⁷

The MIC and MBC values of these compounds against the growth of microorganisms are summarized in table 6. All the structures presented a good antibacterial activity against six bacterial strains. This is attributed to hydrogen bonding between the cellular constituents of the bacterial cell. A small group (Me) for the amino acid gives a best hit (entry 1), whereas moiety offering a supplementary hydrogen bond on the pendant arm does not involve no enhancement (entry 5). It is also concluded that imine and hydroxyl groups play a key role in improving the antibacterial activity.

3. Conclusions

An efficient method for the synthesis of enantiopure imines *via* the condensation of α -amino acid-derived

phenylhydrazides with the 2-hydroxynaphthaldehyde, has been established. These compounds have been characterized by ^1H , ^{13}C -NMR, IR, HRMS, UV-visible spectroscopies and structural X-ray diffraction methods. The first overview of this work is the astonishing non correlation between the environment around the oxygen and the nitrogen atoms of these Schiff bases. Thus, the structure completely behaves neither as an enolate-iminium (III) nor as a keto-amine (II) (figure 5). Secondly, the hydrazone function provides a second intramolecular bonding which deeply impacts the structure. The rigidification is so important that the phenolic form is not obtained in the methanol.

At the solid state, hydrazone function and two intramolecular hydrogen bonds involve a shape close to the planarity for the whole nitrogen- and oxygen- containing region. The freshly prepared Schiff bases have a (*E*)-III form around the nitrogen (i.e. iminium) and an intermediate form between (*E*)-III and (*Z*)-II for the oxygen (figure 5). These very air-stable Schiff bases are able to reveal a solid state reactivity under a slight mechanical treatment converting in part the initial II/III form to the enol-imino I form. The BMK/6-31G(2df,2pd) method and basis sets in the gas phase are adapted to describe the geometry; diffuse functions and dispersion terms damage the geometrical description. The *in-vitro* antibacterial study indicated that the structures **5a-e** exhibited good activities against *Escherichia coli*, *Staphylococcus aureus*, *Candida albicans*, *Salmonella enteridis*, *Pseudomonas* and *Bacillus subtilis*.

4. Experimental

4.1. General comments

All reactions were carried out under an argon atmosphere in round-bottomed flasks equipped with magnetic stirrer. All solvents were freshly distilled before use. Melting points were determined on a Buchi 510 capillary apparatus. NMR spectra were recorded on a Bruker AC 300 spectrometer [300 MHz (^1H) and 75 MHz (^{13}C)]. NMR spectra were calibrated on the non-fully deuterated residual solvent signal (ppm): in DMSO- d_6 at 2.50 (proton) and 39.52 (carbon), in CDCl_3 at 7.26 (proton) and 77.16 (carbon), in MeOD- d_4 at 3.31 (proton) and 49.00 (carbon). Proton and carbon attribution numbers refer to X-ray data (figure 2a) and /or the spectrum section (see ESI). Fourier transformed-IR spectra were recorded on a Nicolet 6700 ATR, to support with Diamond accuracy $\pm 1 \text{ cm}^{-1}$. Electrospray ionisation (ESI) mass spectroscopy data of compounds **5a-e** were recorded on an UPLC Waters device (in positive mode); for the voltages of the mass spectroscopies, the following abbreviations are used: C Capillary (kV), SC Sampling Cone, EC Extraction Cone. Calibration was performed with sodium formate (range from 100 to 1000 $\text{g}\cdot\text{mol}^{-1}$) and the lockspray (lockmass on the leucine encephaline 556.2771 $\text{g}\cdot\text{mol}^{-1}$) was used without collision energy; the relative intensity of peaks is given in brackets. Optical rotations were measured by using a Perkin Elmer Polarimeter (Model 341) using a mercury lamp

(578 nm). UV-Visible spectra were recorded on a Jasco V-530 UV-Visible spectrometer in the range 200-800 nm. Microwave irradiations were realized using a programmed microwave synthesis reactor (START SYNTH, Microwave synthesis Labstation). All biological experiments were performed according to the Guide lines for Animal Experimentation of Monastir University.

4.2. General procedures

Conventional heating

A mixture of 2-hydroxynaphthaldehyde (1.7 g, 10 mmol, 1 eq) and α -aminoacid phenylhydrazide (10 mmol, 1 eq) in methanol (5 mL) was heated under argon at 50 °C for 4 h. The yellow colored precipitate was cooled at room temperature, filtered, washed by cooled methanol and dried in air.

Microwave irradiation

2-hydroxynaphthaldehyde (1.7 g, 10 mmol, 1 eq) was mixed with α -aminoacid phenylhydrazide (10 mmol, 1 eq) in closed vessel and the mixture was irradiated in microwave oven for 5 min at 350 watt. The yellow colored precipitate was filtered, washed by cooled methanol and dried in air. This synthesis processes was performed on a programmed microwave synthesis reactor (START SYNTH).

Ultrasound activation

A mixture of 2-hydroxynaphthaldehyde (1.7 g, 10 mmol, 1 eq) and α -aminoacid phenylhydrazide (10 mmol, 1 eq) in methanol (5 mL) was suggested to ultrasound activation. The yellow colored precipitate was filtered, washed by cooled methanol and dried in air.

4.3. Compound characterization

(*E*)-1-(((1-oxo-1-(2-phenylhydrazinyl)propan-2-yl)iminio)methyl)naphthalen-2-olate (**5a**): Yield 68%. Yellow solid; mp 173-175 °C; R_f 0.16 (EtOAc/ c - C_6H_{12} = 40/60); $[\alpha]_{578} = -26 \pm 3$ (MeCN, $C = 0.078 \pm 0.004$). FT-IR (neat), ν_{max} (cm^{-1}): 3334, 3230, 2981, 1625, 1598; ^1H -NMR (300 MHz, MeOD- d_4): $\delta = 1.69$ (d, 3H, $J = 6.9$ Hz, H24), 4.54 (q, 1H, $J = 6.9$ Hz, H13), 4.62 (brs, 3H, NH15, NH16, H12), 6.73-6.88 (m, 4H, H8, H18, H20, H22), 7.16 (t, 2H, $J = 7.9$ Hz, H19 and H21), 7.26 (t, 1H, $J = 7.6$ Hz, H4), 7.47 (t, 1H, $J = 7.3$ Hz, H3), 7.64 (d, 1H, $J = 7.5$ Hz, H5), 7.78 (d, 1H, $J = 9.3$ Hz, H7), 8.06 (d, 1H, $J = 8.4$ Hz, H2), 9.14 (s, 1H, H11); ^{13}C -NMR (75 MHz, MeOD- d_4): $\delta = 20.40$ (C24), 60.53 (C13), 108.29 (C10), 114.10 (C18 and C22), 119.67 (C2), 121.26 (C20), 124.19 (C4), 125.18 (C8), 127.77 (C6), 129.48 (C3), 130.02 (C19 and C21), 130.23 (C5), 135.47 (C1), 139.57 (C7), 149.71 (C17), 159.72 (C11), 173.15 (C14), 178.13 (C9) ppm; ESI(+)-MS CH_3CN [$C = 0.5$, $SC = 30$, $EC = 3$] m/z (rel. int.): 334 (100, $\text{M} + \text{H}^+$), HRMS ES^+ for $\text{C}_{20}\text{H}_{20}\text{N}_3\text{O}_2$ m/z : [$\text{M} + \text{H}$] $^+$ Calc. 334.1556, found: 334.1553.

(*E*)-1-(((3-methyl-1-oxo-1-(2-phenylhydrazinyl)butan-2-yl)iminio)methyl)naphthalen-2-olate (**5b**): Yield 67%. Yellow solid; mp 179-181 °C; R_f 0.33 (EtOAc/ c - C_6H_{12} = 40/60); $[\alpha]_{578} = -53 \pm 3$ (MeCN, $C = 0.098 \pm 0.004$). FT-IR (neat), ν_{max} (cm^{-1}): 3332, 2969, 2788, 1616, 1595; ^1H -NMR (300 MHz, MeOD- d_4): $\delta = 1.09$ (d, 3H, $J = 7.8$ Hz, Me), 1.11 (d, 3H, $J = 7.8$ Hz, Me), 2.39-2.48 (m, 1H, H24), 4.09 (d, 1H, $J = 6.9$ Hz, H13), 6.78-6.89 (m,

4H, H8, H18, H20 and H22), 7.16 (t, 2H, $J = 7.9$ Hz, H19 and H21), 7.27 (t, 2H, $J = 7.7$ Hz, 1H, H4), 7.46-7.51 (m, 1H, H3), 7.66 (d, 1H, $J = 7.5$ Hz, H5), 7.80 (d, 1H, $J = 9.3$ Hz, H7), 8.06 (d, 1H, $J = 8.4$ Hz, H2), 9.08 (s, 1H, H11); $^1\text{H-NMR}$ (300 MHz, DMSO- d_6): $\delta = 0.99$ (d, 6H, $J = 7.8$ Hz, 2 \times Me), 2.20-2.44 (m, 1H, H24), 3.38 (s, 1H, H12 + H₂O), 4.14-4.18 (m, 1H, H13), 6.61-6.78 (m, 3H, H18, H20 and H22), 6.82 (d, 1H, $J = 9.3$ Hz, H8), 7.13 (t, 2H, $J = 7.3$ Hz, H19 and H21), 7.25 (t, 1H, $J = 7.3$ Hz, H4), 7.48 (t, 1H, $J = 7.5$ Hz, H3), 7.69 (d, 1H, $J = 7.5$ Hz, H5), 7.79 (d, 1H, $J = 9.3$ Hz, H7), 7.91 (s, 1H, NH16), 8.14 (d, 1H, $J = 8.4$ Hz, H2), 9.19 (s, 1H, H11), 10.11 (s, 1H, NH15); $^{13}\text{C-NMR}$ (75 MHz, MeOD- d_4): $\delta = 18.31$ (C25 or C26), 19.64 (C26 or C25), 33.05 (C24), 72.30 (C13), 100.00 (C10), 114.37 (C18 and C22), 119.63 (C2), 121.36 (C20), 124.25 (C4), 124.92 (C8), 127.95 (C6), 129.44 (C3), 129.97 (C19 and C21), 130.25 (C5), 135.45 (C1), 139.33 (C7), 149.79 (C17), 160.46 (C11), 172.22 (C14), 177.63 (C9); $^{13}\text{C-NMR}$ (75 MHz, DMSO- d_6): $\delta = 17.61$ (C25 or C26), 19.08 (C26 or C25), 31.28 (C24), 69.89 (C13), 106.47 (C10), 112.17 (C18 and C22), 118.73 (C20), 118.85 (C2), 122.64 (C4), 124.44 (C8), 125.66 (C6), 128.01 (C3), 128.77 (C19 and C21), 128.98 (C5), 133.91 (C1), 137.00 (C7), 149.18 (C17), 159.45 (C11), 169.48 (C14), 174.99 (C9) ppm; ESI(+)-MS CH₃CN [C= 0.5, SC= 30, EC= 3] m/z (rel. int.): 362 (100, M+H⁺), HRMS ES⁺ for C₂₂H₂₄N₃O₂ m/z : [M+H]⁺ Calc. 362.1860, found: 362.1873.

(E)-1-(((4-methyl-1-oxo-1-(2-phenylhydrazinyl)pentan-2-yl)iminio)methyl)naphthalen-2-olate (**5c**): Yield 70%. Yellow solid; mp 181-183 °C; R_f 0.39 (EtOAc/*c*-C₆H₁₂= 40/60); $[\alpha]_{578} = -68 \pm 6$ (MeCN, C= 0.060 \pm 0.004). FT-IR (neat), ν_{max} (cm⁻¹): 3184, 3024, 2950, 1625, 1546; $^1\text{H-NMR}$ (300 MHz, CDCl₃): $\delta = 0.96$ (d, 6H, $J = 6.0$ Hz), 1.68-1.72 (m, 1H), 1.95 (dd, 2H, $J_1 = 7.5$ Hz, $J_2 = 5.7$ Hz), 4.21-4.26 (m, 1H), 6.81 (d, 2H, $J = 7.8$ Hz), 6.86-6.91 (m, 1H), 7.11-7.22 (m, 4H), 7.36 (t, 1H, $J = 7.8$ Hz), 7.51-7.56 (m, 1H), 7.73-7.84 (m, 2H), 8.01-8.07 (m, 2H), 9.18 (s, 1H), 14.29 (s, 1H); $^1\text{H-NMR}$ (300 MHz, DMSO- d_6): $\delta = 0.97$ (d, 3H, $J = 6.9$ Hz, Me), 0.99 (d, 3H, $J = 6.6$ Hz, Me), 1.51-1.72 (m, 1H, H25), 1.72-1.94 (m, 2H, H24), 3.38 (s, 1H, H12), 4.40-4.54 (m, 1H, H13), 6.66-6.76 (m, 3H, H18, H20 and H22), 6.83 (d, 1H, $J = 9.3$ Hz, H8), 7.12 (t, 2H, $J = 8.2$ Hz, H19 and H21), 7.26 (t, 1H, $J = 7.2$ Hz, H4), 7.49 (t, 1H, $J = 7.2$ Hz, H3), 7.70 (d, 1H, $J = 7.8$ Hz, H5), 7.80 (d, 1H, $J = 9.6$ Hz, H7), 7.90 (s, 1H, NH16), 8.15 (d, 1H, $J = 8.4$ Hz, H2), 9.26 (d, 1H, $J = 6.3$ Hz, H11), 10.14 (s, 1H, NH15); $^{13}\text{C-NMR}$ (75 MHz, CDCl₃): $\delta = 21.35$, 23.07, 24.59, 43.01, 69.52, 108.41, 113.76, 118.98, 120.80, 121.43, 123.64, 127.57, 128.16, 129.17, 129.30, 132.84, 136.05, 147.71, 162.16, 166.48, 171.51; $^{13}\text{C-NMR}$ (75 MHz, DMSO- d_6): $\delta = 21.95$ (C26 or C27), 22.70 (C27 or C26), 24.42 (C25), 41.86 (C24), 62.75 (C13), 106.64 (C10), 112.14 (C18 and C22), 118.73 (C20), 118.93 (C2), 122.71 (C4), 124.08 (C8), 125.78 (C6), 127.99 (C3), 128.75 (C19 and C21), 128.98 (C5), 133.76 (C1), 136.86 (C7), 149.09 (C17), 159.22 (C11), 170.07 (C14), 174.15 (C9) ppm; ESI(+)-MS CH₃CN [C= 0.5, SC= 30, EC= 3] m/z (rel. int.): 376 (100, M+H⁺), HRMS ES⁺ for C₂₃H₂₆N₃O₂ m/z : [M+H]⁺ Calc. 376.2025, found: 376.2028.

(E)-1-(((1-oxo-3-phenyl-1-(2-phenylhydrazinyl)propan-2-yl)iminio)methyl)naphthalen-2-olate (**5d**): Yield 56%. Yellow solid; mp 197-199 °C; R_f 0.35 (EtOAc/*c*-C₆H₁₂= 40/60); $[\alpha]_{578} = -180 \pm 11$ (MeCN, C= 0.068 \pm 0.004). FT-IR (neat), ν_{max} (cm⁻¹):

3341, 3021, 2746, 1617, 1545; $^1\text{H-NMR}$ (300 MHz, MeOD- d_4): $\delta = 3.22$ (dd, 1H, $J = 13.3$, 7.9 Hz, H24), 3.44 (dd, 1H, $J = 13.2$, 6.9 Hz, H24), 4.59 (t, 1H, $J = 7.5$ Hz, H13), 6.59 (d, 2H, $J = 7.5$ Hz, H18 and H22), 6.77 (t, 1H, $J = 7.2$ Hz, H20), 6.85 (d, 1H, $J = 9.3$ Hz, H8), 7.10 (t, 2H, $J = 7.9$ Hz, H19 and H21), 7.15-7.30 (m, 4H, H4, H27, H28, H29), 7.30-7.36 (m, 3H, H26, H30), 7.41 (t, 1H, $J = 7.8$ Hz, H3), 7.63 (d, 1H, $J = 7.8$ Hz, H5), 7.78 (t, 2H, $J = 8.5$ Hz, H2, H7), 8.78 (s, 1H, H11); $^{13}\text{C-NMR}$ (75 MHz, MeOD- d_4): $\delta = 41.42$ (C24), 67.64 (C13), 108.23 (C10), 114.09 (C18 and C22), 119.59 (C2), 121.16 (C20), 124.19 (C4), 124.75 (C8), 128.28 (C6), 129.32 (C3), 129.85 (C19, C21 and C28), 129.94 (C27 and C29), 130.19 (C5), 130.88 (C25), 130.95 (C26 and C30), 137.40 (C1), 139.29 (C7), 149.46 (C17), 160.13 (C11), 171.92 (C14), 177.02 (C9); ESI(+)-MS CH₃CN [C= 0.5, SC= 30, EC= 3] m/z (rel. int.): 410 (100, M+H⁺), HRMS ES⁺ for C₂₆H₂₄N₃O₂ m/z : [M+H]⁺ Calc. 410.1869, found: 410.1872.

(E)-1-(((3-hydroxy-1-oxo-1-(2-phenylhydrazinyl)propan-2-yl)iminio)methyl)naphthalen-2-olate (**5e**): Yield 73%. Yellow solid; mp 206-207 °C; R_f 0.1 (EtOAc/*c*-C₆H₁₂= 40/60); $[\alpha]_{578} = -26 \pm 4$ (MeCN, C= 0.060 \pm 0.004). FT-IR (neat), ν_{max} (cm⁻¹): 3024, 2849, 1693, 1625; $^1\text{H-NMR}$ (300 MHz, MeOD- d_4): $\delta = 4.00$ (dd, 1H, $J_1 = 10.8$ Hz, $J_2 = 6.9$ Hz), 4.10 (dd, 1H, $J_1 = 10.8$ Hz, $J_2 = 5.1$ Hz), 4.45-4.49 (m, 1H), 6.81-6.89 (m, 5H), 7.15-7.27 (m, 4H), 7.45-7.50 (m, 1H), 7.65 (d, 1H, $J = 7.8$ Hz), 7.78 (d, 1H, $J = 9.00$ Hz), 8.06 (d, 1H, $J = 8.4$ Hz), 9.14 (s, 1H); $^1\text{H-NMR}$ (300 MHz, DMSO- d_6): $\delta = 3.71$ -3.86 (m, 1H, H24), 3.86-4.00 (m, 1H, H24), 4.46 (dd, 1H, $J = 11.2$, $J = 5.8$ Hz, H13), 5.33-5.47 (m, 1H, OH), 6.65-6.85 (m, 4H, H8, H18, H20 and H22), 7.13 (t, 2H, $J = 7.8$ Hz, H19 and H21), 7.23 (t, 1H, $J = 7.3$ Hz, H4), 7.47 (t, 1H, $J = 7.2$ Hz, H3), 7.67 (d, 1H, $J = 7.5$ Hz, H5), 7.77 (d, 1H, $J = 9.3$ Hz, H7), 7.86 (d, 1H, $J = 1.8$ Hz, NH16), 8.08 (d, 1H, $J = 8.4$ Hz, H2), 9.12 (d, 1H, $J = 8.7$ Hz, H11), 10.09 (d, 1H, $J = 1.8$ Hz, NH15); $^{13}\text{C-NMR}$ (75 MHz, MeOD- d_4): $\delta = 64.36$, 68.08, 108.71, 113.99, 114.35, 119.78, 121.34, 124.22, 124.79, 128.01, 129.39, 129.98, 130.20, 135.45, 139.19, 139.79, 149.63, 161.17, 171.06, 176.82, $^{13}\text{C-NMR}$ (75 MHz, DMSO- d_6): $\delta = 62.83$ (C24), 65.65 (C13), 106.43 (C10), 112.26 (C18 and C22), 118.72 (C2 and C20), 122.53 (C4), 124.75 (C8), 125.58 (C6), 128.00 (C3), 128.75 (C19 and C21), 128.98 (C5), 134.08 (C1), 137.06 (C7), 149.98 (C17), 159.33 (C11), 168.37 (C14), 175.47 (C9) ppm; ESI(+)-MS CH₃CN [C= 0.5, SC= 30, EC= 3] m/z (rel. int.): 350 (100, M+H⁺), HRMS ES⁺ for C₂₀H₂₀N₃O₃ m/z : [M+H]⁺ Calc. 350.1505, found: 350.1510.

Conflicts of interest

There are no conflicts to declare.

Acknowledgements

The authors thank the DGRSRT (Direction Générale de la Recherche Scientifique et de la Rénovation Technologique) of the Tunisian Ministry of Higher Education and Scientific research and Technology for financial support of this research.

Notes and references

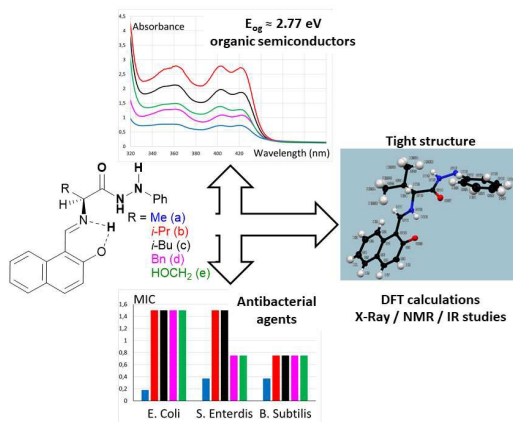
- H. Schiff, *Euro. J. Org. Chem.*, 1864, **131**, 9–118.
- M. Enamullah, A. B. Uddin, G. Pescitelli, R. Berardozi, G. Makhloufi, V. Vasylyeva, A. C. Chamayou and C. Janiak, *Dalton Trans.*, 2014, **43**, 3313–3329.
- M. Enamullah, V. Vasylyeva and C. Janiak, *Inorg. Chim. Acta.*, 2013, **408**, 109–119.
- S. Y. Ebrahimipour, I. Sheikhshoae, A. Crochet, M. Khaleghi and M. K. Fromm, *J. Mol. Struct.*, 2014, **1072**, 267–276.
- K. C. Gupta and A. K. Sutar, *Coord. Chem. Rev.*, 2008, **252**, 1420–1450.
- M. Rezaeivala and H. Keypour, *Coord. Chem. Rev.*, 2014, **280**, 203–253.
- C. Cimarelli and G. Palmieri, *Tetrahedron*, 2000, **56**, 475–478.
- C. P. Singh and H. Hasan, *Asian J. Chem.*, 2003, **15**, 49–52.
- A. Song, X. Wang and K. S. Lam., *Tetrahedron Lett.*, 2003, **44**, 1755–1758.
- K. Neuvonen and K. Pihlaja, *J. Chem. Soc. Perkin Trans.*, 1988, 461–467.
- V. Y. Korotaev, V. Y. Sosnovskikh, I. B. Kutyashev, A. Y. Barkov, E. G. Matochkina and M. I. Kodess, *Tetrahedron*, 2008, **64**, 5055–5060.
- M. S. Y. Khan, R. M. Khan and S. Drabu, *Indian. J. Heterocycl. Chem.*, 2001, **11**, 119–122.
- S. Cao, X. Qian, G. Song and Q. Huang, *J. Fluorine Chem.*, 2002, **117**, 63–66.
- S. M. Seyedi, R. Sandaroods and G. H. Zohuri, *Chin. Chem. Lett.*, 2010, **21**, 1303–1306.
- L. Yin, X. Jia and X. S. Li, *Chin. Chem. Lett.*, 2010, **21**, 774–777.
- Y. L. Yang, N. N. Wan, M. P. Wang, Z. F. Xie and J. D. Wang, *Chin. Chem. Lett.*, 2011, **22**, 1071–1074.
- K. Yamaguchi, S. Koshino, F. Akagi, M. Suzuki, A. Uehara and S. Suzuki, *J. Am. Chem. Soc.*, 1997, **119**, 5752–5753.
- T. M. Krygowski, K. Wozniak, R. Anulewicz, D. Pawlak, W. Kolodziejewski, E. Grech and A. Szady, *J. Phys. Chem.*, 1997, **101**, 9399–9404.
- O. Dominguez, B. Rodriguez, M. Rodriguez, A. Ariza, N. Farfan and R. Santillan, *New J. Chem.*, 2011, **35**, 156–164.
- R. Pis-Diez, G. A. Echeverria, O. E. Piro, J. L. Jios and B. S. Parajon-Costa, *New J. Chem.*, 2016, **40**, 2730–2740.
- P. M. Dominiak, E. Grech, G. Barr, S. Teat, P. Mallinson and K. Wozniak, *Chem. Eur. J.*, 2003, **9**, 963–970.
- A. C. González-Baró, R. Pis-Diez, B. S. Parajón-Costa and N. A. Rey, *J. Mol. Struct.*, 2012, **1007**, 95–101.
- H. Pizzala, M. Carles, W. E. E. Stone and A. Thevand, *J. Chem. Soc., Perkin Trans.*, 2000, **2**, 935–939.
- A. Filarowski, A. Koll, T. Glowiak, E. Majewski and T. Dziembowska, *Ber. Bunsen-Ges. Phys. Chem.*, 1998, **102**, 393–397.
- K. Ogawa and J. Harada, *J. Mol. Struct.*, 2003, **647**, 211–216.
- M. Rubcic, K. Uzarevic, I. Halasz, N. Bregovic, M. Malis, I. Dilovic, Z. Kokan, R. S. Stein, R. E. Dinnebie and V. Tomisic, *Chem. Eur. J.*, 2012, **18**, 5620–5631.
- S. D. Chatziefthimiou, Y. G. Lazarou, E. Hadjoudis, T. Dziembowska and I. M. Mavridis, *J. Phys. Chem.*, 2006, **47**, 23701–23709.
- Y. Kacem and B. Ben Hassine, *Tetrahedron: Asymmetry*, 2014, **25**, 252–257.
- Y. Kacem and B. Ben Hassine, *Heterocycles*, 2014, **89**, 197–207.
- G. Verardo, N. Toniutti, A. Gorassini and A. G. Giumanini, *Eur. J. Org. Chem.*, 1999, 2943–2948.
- a) G. M. Sheldrick, SADABS, program for scaling and correction of area detector data, University of Göttingen, Germany, 1997; b) R. Blessing, *Acta Cryst.*, 1995, **A51**, 33–38; c) G. M. Sheldrick, *Acta Cryst.*, 1990, **A46**, 467–473; d) G. M. Sheldrick, SHELX-TL version 5.03, Software Package for the Crystal Structure Determination, Siemens Analytical X-ray Instrument Division : Madison, WI USA, 1994; e) these data can be obtained free of charge via www.ccdc.cam.ac.uk/data_request/cif; $C_{22}H_{23}N_3O_2$, $M_w = 361.43$, orthorhombic, space group $P2_12_12_1$; dimensions: $a = 10.3964(5) \text{ \AA}$, $b = 10.8708(5) \text{ \AA}$, $c = 17.5190(7) \text{ \AA}$, $V = 1979.95(15) \text{ \AA}^3$; $Z = 4$; $D_x = 1.213 \text{ Mg m}^{-3}$; $\mu = 0.08 \text{ mm}^{-1}$; 117330 reflections measured at 200 K; independent reflections: 5839 [$5372 F_o > 4\sigma(F_o)$]; data were collected up to a $2\theta_{max}$ value of 60.2° (99.8 % coverage). Number of variables: 258; $R_1 = 0.0345$, $wR_2 = 0.0903$, $S = 1.048$; highest residual electron density 0.24 e. \AA^{-3} ; CCDC = 1577687; f) C. F. Macrae, I. J. Bruno, J. A. Chisholm, P. R. Edgington, P. McCabe, E. Pidcock, L. Rodriguez-Monge, R. Taylor, J. van de Streek and P. A. Wood, *J. Appl. Cryst.*, 2008, **41**, 466–470.
- Usual bond values (\AA) for molecular solids are 1.22 (C=O), 1.43 (C-O), then 1.30 (C=N), 1.47 (C-N).
- P. Hande, C. Albayrak, O. Mustafa, S. Ismet and B. Orhan, *J. Chem Crystallogr.*, 2008, **38**, 901–905.
- H. Karabiyik, I.N. Ocaik, H. Petek, C. Albayrak and E. Ađar, *J. Mol. Struct.*, 2008, **873**, 130.
- M. Juribasic, N. Bregovic, V. Stilianovic, V. Tomisic, M. Cindric, P. Sket, J. Plavec, M. Rubcic and K. Uzarevic, *Chem. Eur. J.*, 2014, **20**, 17333–17345.
- G. O. Dudek and G. P. Volpp, *J. Am. Chem. Soc.*, 1963, **85**, 2697–2702.
- P. Przybylski, W. Lewandowska, B. Brzezinski and F. Bartl, *J. Mol. Struct.*, 2006, **797**, 92–98.
- For Schiff bases, ^1H NMR usual chemical shifts (ppm) are the following in deuterated solvents at rt: a) C-OH phenolic proton 13.7–14.0 (DMSO, ref 22, 27, 35), 14.1 (DMF, ref 35) 12.7 (CDCl₃, ref 35), 13.3 (MeCN, ref 35); b) N-H...O=C 10–12 (DMSO, ref 22); c) HC=N...H-O iminomethine proton 8.3–8.9 (DMSO, ref 18, 22, 27), 9.4–9.5 (DMSO or MeCN or CDCl₃ or DMF, ref 35), 9.3 (MeOD, ref 35).
- For Schiff bases, ^{13}C NMR usual chemical shifts (ppm) are the following in deuterated solvents at rt: a) C-OH phenolic carbon 152.8 (DMSO, ref 22), 167 (CDCl₃, ref 19), 160 (MeOD or MeCN, ref 26); b) C=O quinodic carbon 178 (DMSO, ref 24), 172 (CDCl₃, ref 24); c) C-N iminomethine carbon 166 (DMSO, ref 24), 164 (CDCl₃, ref 24).
- C. Abbas-Quinternet, PhD thesis, *Synthèse et études structurales de nouveaux 2:1-[α /aza]-oligomères, vers de nouveaux foldamères*, Nancy Université, Institut National Polytechnique de Lorraine, 5 octobre 2009, p.132–157, free access online.
- For the enol-imine form Schiff bases, the following values (cm^{-1}) in literature are reported (ns= neat solid): a) C=N [ν] 1641 (ns, ref 22), 1627–1614 (ref 19), 1607–1606 (KBr, ref 26, 18), 1554 (KBr, ref 26); b) O-H [ν] 3441–3316 (ref 19), 2996 (ns, ref 22), 2441–2434 (KBr, ref 26), $[\delta]$ 1388–1381 (ns, ref 22), 1388–1374 (KBr, ref 18), $[\gamma_{o-o-p}]$ 839–838 (KBr, ref 18), 809 (ns, ref 22); c) C-O [ν] 1343–1327 (ns, ref 22), 1327–1324 (KBr, ref 18).
- For the keto-amine form Schiff bases, the following values (cm^{-1}) in literature are reported (ns= neat solid): a) N-H [ν] 3469–3458, 3362–3318 (KBr, ref 35), 3221 (ns, ref 22), 3214–3053 (ref 19), 2858 (KBr, ref 35), 2631–2626 (KBr, ref 35), 2538–2520 (KBr, ref 26, 35), $[\gamma_{o-o-p}]$ 878 (ns, ref 22); b) C=O [ν] 1662 (KBr, ref 35), 1657–1639 (ref 19), 1645 (ns, ref 22), 1623–1617 (KBr, ref 26, 35), 1525–1516 (KBr, ref 26).
- a) According to our previous published works^{28,29} C=O bands of **3a-e** compounds in KBr are (cm^{-1}): 1665, 1655, 1661, 1648, 1680 respectively; b) the reference 40 gives (cm^{-1}) for CO-NR-NHR H 1779–1746 (in H bonding), 1729–1705 (free), for CO-NR-N=C 1705, for CO-NH-NRR' 1725.
- Gaussian 09, Revision D.01, M. J. Frisch, G. W. Trucks, H. B. Schlegel, G. E. Scuseria, M. A. Robb, J. R. Cheeseman, G.

- Scalmani, V. Barone, B. Mennucci, G. A. Petersson, H. Nakatsuji, M. Caricato, X. Li, H. P. Hratchian, A. F. Izmaylov, J. Bloino, G. Zheng, J. L. Sonnenberg, M. Hada, M. Ehara, K. Toyota, R. Fukuda, J. Hasegawa, M. Ishida, T. Nakajima, Y. Honda, O. Kitao, H. Nakai, T. Vreven, J. A. Montgomery, Jr., J. E. Peralta, F. Ogliaro, M. Bearpark, J. J. Heyd, E. Brothers, K. N. Kudin, V. N. Staroverov, R. Kobayashi, J. Normand, K. Raghavachari, A. Rendell, J. C. Burant, S. S. Iyengar, J. Tomasi, M. Cossi, N. Rega, J. M. Millam, M. Klene, J. E. Knox, J. B. Cross, V. Bakken, C. Adamo, J. Jaramillo, R. Gomperts, R. E. Stratmann, O. Yazyev, A. J. Austin, R. Cammi, C. Pomelli, J. W. Ochterski, R. L. Martin, K. Morokuma, V. G. Zakrzewski, G. A. Voth, P. Salvador, J. J. Dannenberg, S. Dapprich, A. D. Daniels, O. Farkas, J. B. Foresman, J. V. Ortiz, J. Cioslowski and D. J. Fox, *Gaussian, Inc.*, Wallingford CT, 2009.
- 45 a) A. D. Becke, *J. Chem. Phys.*, 1993, **98**, 5648–5652; b) C. Lee, W. Yang and R. G. Parr, *Phys. Rev. B*, 1988, **37**, 785–789.
- 46 Y. Zhao and D. G. Truhlar, *J. Phys. Chem.*, 2006, **110**, 5121–5129.
- 47 T. Yanai, D. Tew and N. Handy, *Chem. Phys. Lett.*, 2004, **393**, 51–57.
- 48 a) J. P. Perdew, K. Burke and M. Ernzerhof, *Phys. Rev. Lett.*, 1996, **77**, 3865–3868; b) J. P. Perdew, K. Burke and M. Ernzerhof, *Phys. Rev. Lett.*, 1997, **78**, 1396; c) C. Adamo and V. Barone, *J. Chem. Phys.*, 1999, **110**, 6158–6169.
- 49 J.-D. Chai and M. Head-Gordon, *Phys. Chem. Chem. Phys.*, 2008, **10**, 6615–6620.
- 50 J. P. Perdew, *Phys. Rev. B*, 1986, **33**, 8822–8824.
- 51 A. D. Boese and J. M. L. Martin, *J. Chem. Phys.*, 2004, **121**, 3405–3416.
- 52 T. H. Dunning Jr. and P. J. Hay, in *Modern Theoretical Chemistry*, Ed. H. F. Schaefer III, (Plenum, New York, 1976, **3**, 1–28.
- 53 R. S. Mulliken, *J. Chem. Phys.*, 1955, **23**, 1833–1840.
- 54 NBO Version 3.1, E. D. Glendening, A. E. Reed, J. E. Carpenter, F. Weinhold, *Gaussian Link 607*.
- 55 C. M. Breneman and K. B. Wiberg, *J. Comp. Chem.*, 1990, **11**, 361–373.
- 56 a) B. H. Besler, K. M. Jr. Merz and P. A. Kollman, *J. Comp. Chem.*, 1990, **11**, 431–439; b) U. C. Singh and P. A. Kollman, *J. Comp. Chem.*, 1984, **5**, 129–145.
- 57 R. Koster, M. Anderson and E. J. De Beer, *Fed. Proc.*, 1959, **18**, 418–420.

Enantiopure Schiff bases of aminoacid phenylhydrazides: impact of the hydrazone function on their structure and properties

Nadia Bouzayani, Sylvain Marque, Brahim Djelassi, Yakdhane Kacem, Jérôme Marrot and Béchir Ben Hassine

A new chiral Schiff bases have been synthesized and characterized with an important contribution of quantum chemical calculations at a DFT level of theory. They have been evaluated for their physical and biological properties.



The article was first published on date

New J. Chem., 2018, 42, Paper